Acuracy and Reliability of Post-Processing Software for DSC MR Perfusion: Quantitative Analysis by Digital Phantom Data

K. Kudo[1], S. Christensen[2], M. Sasaki[1], M. Straka[3], S. Fujiwara[1], K. Ishizaka[4], Y. Zaitsu[4], N. Fujima[4], S. Terae[4], K. Ogasawara[5], and L. Ostergaard[6]

[1]Advanced Medical Research Center, Iwate Medical University, Morioka, Iwate, Japan, [2]Departments of Neurology and Radiology, University of Melbourne, Melbourne, Australia, [3]Department of Radiology, Stanford University, California, United States, [4]Department of Radiology, Hokkaido University Hospital, Sapporo, Japan, [5]Department of Neurosurgery, Iwate Medical University, Morioka, Iwate, Japan, [6]Department of Neuroradiology, Aarhus University Hospital, Aarhus, Denmark

Purpose:

A variety of post-processing programs and algorithms for dynamic susceptibility contrast (DSC) MR perfusion are available from MR manufacturers, third-party workstation vendors, and academic groups. However, the accuracy and reliability of these programs have not been subject to standardized quality control. The purposes of this study were (1) to design a digital phantom data set for DSC MR perfusion based on widely accepted tracer kinetic theory in which a range of true values of cerebral blood flow (CBF), cerebral blood volume (CBV), mean transit time (MTT), and tracer arrival delay are known, and (2) to evaluate the accuracy of post-processing programs using this digital phantom.

Materials and Methods:

The phantom data set was created by generating concentration time curves (CTC) reflecting CBF ranging from 5 to 70 mL/min/100g, MTT ranging from 3.4 to 24 s, and CBV of 2% and 4%. Tracer delays up to +/- 3 seconds were also introduced. Linear, boxcar, and exponential residue functions were used. The CTCs were converted to signal-time curves, and noise was added to both the real and complex part of this signal. In total, the phantom contains 294 unique combinations of CBV, CBF and delay, each represented with 1024 different noise realizations in quadratic blocks (Fig. 1 and 2). The phantom was then stored in DICOM format.

This phantom data was analyzed with 3 commercially available software packages (GE healthcare, Hitachi Medical Systems, and Siemens Medical Systems), and 4 academic programs (Perfusion Mismatch Analyzer (PMA), Rapid, Penguin, and EPITHET). Two of them (GE and Hitachi) used non-deconvolution based algorithms (gamma-fitting and first moment MTT), and the rest of them used deconvolution by singular value decomposition (SVD) of standard type (sSVD) or circular type (cSVD). CBF, CBV, and MTT maps were generated, and Tmax map was also created by deconvolution programs. Region-of-interest (ROI) measurements were performed on these maps. Sensitivity for tracer arrival delay in CBF, CBV and MTT was evaluated by coefficient of variation (CV) against different delay time. Linearity of CBF or MTT was also evaluated by correlation coefficient between measured values and true values. Dependency of CBV on true MTT was assessed by CV. Correlations between Tmax and delay or true MTT, were also calculated.

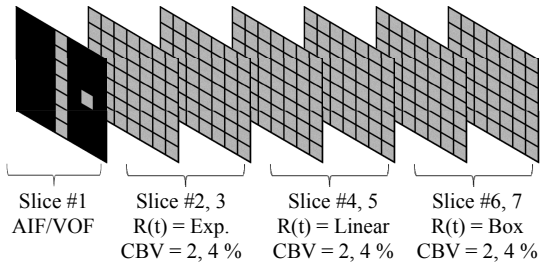

Fig 1. Data Structure of Digital Phantom.
The phantom data set has 7 slices and 50 phases (total 350 images). Signals for AIF/VOF are embedded in slice #1. Tissue curves are embedded in slice #2 to #7, with different R(t) and CBV.

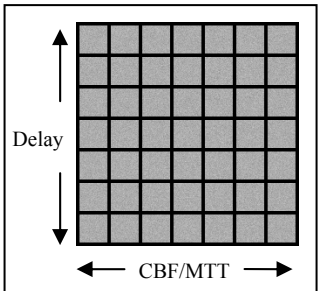

Fig 2. Tissue Slice.
Each tissue slice has 7 x 7 tiles, each of which has different combination of CBF/MTT and delay.

Results:

Average CV value of CBF against delay were larger in sSVD (PMA, 29.6%; Rapid, 28.5%; Penguin, 28.0%; EPITHET 27.7%; and Siemens, 26.1%) than cSVD (PMA, 3.0%; Rapid, 1.6%; and Penguin, 2.6%) and gamma-fitting method (GE, 4.8%; and Hitachi, 0.8%). CVs of MTT were also larger in sSVD (PMA, 31.5%; Rapid, 28.1%; Penguin, 46.6%; EPITHET, 27.5%; and Siemens, 32.6%) than in cSVD (PMA, 3.2%; Rapid, 1.9%; and Penguin, 21.9%) and gamma-fitting method (GE, 4.6%, Hitachi, 2.1%). CVs of CBV were small in most programs (PMA, 0.6%; Rapid, 0.7%; Penguin, 20.7%; EPITHET, 0.8%; GE, 2.1%; Hitachi, 0.5%; and Siemens, 0.6%).

Correlation coefficient between measured CBF and true CBF was larger in all deconvolution methods ($r > 0.98$) than in gamma-fitting (GE, $r = 0.95$; and Hitachi, $r = 0.95$). Correlation between measured MTT and true MTT was also larger in all deconvolution methods ($r > 0.99$) than in gamma-fitting (GE, $r = 0.96$; Hitachi, $r = 0.95$). In addition, all academic software produced similar MTT values against true MTT.

Dependency of CBV on true MTT was relatively low but varied among software in terms of CVs (PMA, 5.7%; Rapid, 1.5%; Penguin, 5.1%; EPITHET, 1.3%; GE, 13.0%; Hitachi, 9.1%; and Siemens, 1.6%).

Linearity of Tmax against delay was generally good, and correlation coefficient was higher in cSVD (PMA, 0.96; Rapid, 0.97; and Penguin, 0.98) than in sSVD (PMA, 0.95; Rapid, 0.89; Penguin, 0.90; and EPITHET, 0.92). Dependency of Tmax against true MTT was large in most programs ($r > 0.94$).

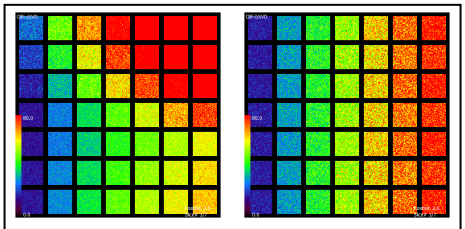

Fig 3. Example of CBF Maps Analyzed by PMA. CBF values are affected by delay in standard SVD (left). However, the delay-dependency is not observed in block-circulant SVD (right). Linearity of CBF is also different between these two techniques.

Conclusions:

By using this phantom, we could confirm that circular SVD produced delay-insensitive results compared to the standard SVD algorithm, and linearity on CBF and MTT against true values was better in deconvolution based programs than in non-deconvolution based programs. A Digital phantom is a useful tool for the evaluation of accuracy and characteristics of quantitative values derived from DSC perfusion analysis software.

References:

1. Wintermark M, et al: Acute stroke imaging research roadmap. Stroke 2008;39:1621-1628..
2. Ostergaard L: Principles of cerebral perfusion imaging by bolus tracking. J Magn Reson Imaging 2005;22:710-717.
3. Wu O, et al: Tracer arrival timing-insensitive technique for estimating flow in MR perfusion-weighted imaging using singular value decomposition with a block-circulant deconvolution matrix. Magn Reson Med 2003;50:164-174.
4. Kudo K, et al: Difference in tracer delay-induced effect among deconvolution algorithms in ct perfusion analysis: Quantitative evaluation with digital phantoms. Radiology 2009;251:241-249.